

Phase Diagram of Yukawa Systems: Model for Charge-Stabilized Colloids

Kurt Kremer,^(a) Mark O. Robbins,^(b) and Gary S. Grest

Corporate Research Science Laboratories, Exxon Research and Engineering Company, Annandale, New Jersey 08801

(Received 29 August 1986)

The phase diagram of particles interacting through a repulsive screened Coulomb (Yukawa) potential has been calculated. Such interactions describe charge-stabilized colloidal suspensions and provide a potential of variable shape which can be used to test general ideas about phase transitions, including the phenomenological Hansen-Verlet and Lindemann rules. Competition between bcc and fcc solid phases was explored through calculations of the free-energy difference. For a range of screening lengths we found a transition from a low-temperature fcc phase to a high-temperature bcc phase.

PACS numbers: 64.70.Dv, 64.70.Kb, 82.70.Dd

Many physical systems with screened Coulomb interactions can be described by repulsive Yukawa interparticle potentials. One class of examples are dilute charge-stabilized colloidal suspensions such as latex spheres in water, micelles, and microemulsions.¹ Recently, such suspensions have been found to form a variety of crystalline, amorphous, and liquid phases. Both equilibrium¹ and nonequilibrium^{1,2} phase transitions have been observed.

In this paper, we present a study of the phase diagram of repulsive Yukawa systems using molecular dynamics (MD). In addition to describing a variety of real physical systems, Yukawa systems provide a testing ground for general ideas about phase transitions because the shape of the potential varies continuously with the screening length κ^{-1} . We compare our results with the Hansen-Verlet³ and Lindemann⁴ criteria for the melting transition over a wide range of screening lengths. In the solid phase, we study the relative stability of the fcc and bcc structures. The range of stability of the bcc phase increases substantially as T increases. Transitions from fcc to bcc with increasing T are found in many elemental metals.⁵

The energy per particle of a system of N particles interacting with a repulsive Yukawa potential is

$$U = \frac{1}{2N} U_0 \sum_{i,j} (a/r_{ij}) \exp(-\lambda r_{ij}/a), \quad (1)$$

where the sum is over all pairs of particles ij , U_0 is a measure of the interaction strength, and $\lambda = \kappa a$. Here a is the natural length scale, $a \equiv n^{1/3}$ and n is the number density. For point particles with charge Z and Debye-Hückel screening: $U_0 = Z^2 e^2 / \epsilon a$ and $\kappa^2 = 4\pi n Z e^2 / \epsilon k_B T$, where ϵ is the dielectric constant of the medium. In general the particles have finite size and the screening is not described by the linearized Debye-Hückel equations. However, as shown by Alexander *et al.*,⁶ the potential can still be described in terms of an effective charge and screening length.

It is convenient to define a dimensionless temperature

$$\tilde{T} \equiv k_B T / (M \omega_E^2 a^2), \quad (2)$$

where M is the particle mass and ω_E is the Einstein frequency: the frequency of a single particle moving with all other particles held fixed on a lattice. For a general lattice $\omega_E^2 = \langle \omega^2 \rangle$, the mean squared phonon frequency. For the Yukawa potential⁷

$$M \omega_E^2 a^2 = 2\lambda^2 U(\lambda) / 3, \quad (3)$$

where $U(\lambda)$ is the energy given by Eq. (1) with all particles at lattice sites. While we use ω_E for the fcc lattice to define \tilde{T} , it differs by at most 0.1% from the value for the bcc lattice over the range of λ where the two structures compete.

The stable phase of a Yukawa system depends only on the dimensionless parameters λ and \tilde{T} . The phase diagram is presented in Fig. 1. Since the interactions are completely repulsive, there is no distinction between liquid and gas phases. Both experiments on colloidal

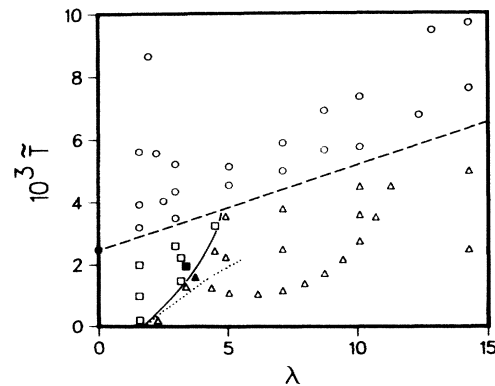


FIG. 1. The phase diagram of Yukawa systems. Open circles indicate points where the liquid phase was stable. Points where the fcc and bcc solid phases are stable are indicated by open triangles and open squares, respectively. The solid square and solid triangle indicate cases that crystallized from the melt. The dashed line separating liquid and solid phases indicates the value of \tilde{T} where the rms displacement reaches 19% of a . The dotted line is the harmonic result for the bcc to fcc phase transition, and the solid line interpolates our MD results for this transition.

suspensions and our simulations are performed at constant volume.

For $\tilde{T}=0$, the stable phase is determined by minimization of the total energy [Eq. (1)]. For the Coulomb limit, $\lambda=0$, the bcc structure is stable (the well-known Wigner lattice). As λ increases, the range of the potential decreases and nearest-neighbor interactions become increasingly important. For $\lambda > \lambda_c = 1.72$ the fcc structure becomes stable because the nearest-neighbor distance is larger than in a bcc lattice of the same density.⁷ The number of nearest neighbors becomes irrelevant for large λ because of the exponential falloff of the potential. The behavior at finite \tilde{T} for $\lambda=0$ has been studied previously with the Monte Carlo (MC) method.⁸ Pollock and Hansen found a melting transition at $\tilde{T}=0.0025 \pm 0.0002$ which is indicated in Fig. 1.

We have filled in the remainder of the phase diagram using MD simulations of between 432 and 588 particles with periodic boundary conditions. A fifth-order predictor-corrector algorithm was used to integrate the equations of motion with a time step, $\Delta t \cong 0.06\omega_E^{-1}$. The interaction potential was truncated at $r_c = 3.07a$. Pollock and Hansen used smaller systems but evaluated the full Ewald sum for $\lambda=0$. We have studied the effect of r_c and particle number on our MD results and lattice-dynamics calculations.⁹ Finite size effects in 500 particle systems are of the order of 10% for all λ . The effects of finite r_c become larger for $\lambda < 2$. For small λ , Ewald sums or larger systems are needed for accurate phase-diagram calculations.

In Fig. 1, open circles indicate points where crystalline starting states melted within $\sim 9000\Delta t$. These points represent an upper bound for the melting transition because of the finite run times, and hysteresis in the first-order melting transition. Pollock and Hansen's analysis,⁸ based on MC and analytic fits to the free energy of solid and liquid phases, suggests that the melting temperature may be about 15% below these points. Crystallization of supercooled liquid starting states was much slower. Only two runs crystallized and each took about $50000\Delta t$. One run crystallized into the bcc phase and the other into the fcc. These points are indicated by the solid square and solid triangle, respectively, in Fig. 1.

Given the long times needed to crystallize our systems from the melt, two other methods for determining the solid-solid phase boundary were tried. Since fcc and bcc structures are related by a simple shear, transitions between them may occur rapidly in constant-pressure simulations.¹⁰ However, for Yukawa systems there is a substantial region where both structures are metastable and no transition was seen within our runs. Therefore, the phase boundary was determined by calculation of the free-energy difference following Rahman and Jacucci.¹¹ In Fig. 1 the points where the fcc and bcc structures were found to have the lowest free energy are indicated by open triangles and open squares, respectively. Very

near melting, our free-energy results could be checked with standard MD runs: The stable phase was found to be solid at temperatures where the other phase melted. The region of bcc stability increases with increasing \tilde{T} . It is interesting to compare this behavior with the phase diagrams of elemental metals. At atmospheric pressure the low- T phase of most elemental metals is either close-packed (fcc or hcp) or bcc. As T increases some elements melt without intermediate phase transitions, but many close-packed elements transform to the bcc phase before melting.⁵ As a function of λ one finds the whole variety of phase behavior observed for elemental metals.

Several attempts have been made to construct general arguments for the increased stability of the bcc phase as T is increased. Alexander and McTague¹² constructed a Ginzburg-Landau theory which suggests that the bcc phase should always be stable just below the melting curve if the transition is weakly first order. However, this cannot be true for Yukawa systems because the bcc structure is unstable against shear for $\lambda > 7.67$. Even low- T runs for $\lambda > 7.67$ show a rapid transformation from the bcc to a distorted close-packed structure. It is known¹³ that the bcc structure is unstable against shear for other stiff potentials: repulsive r^{-n} potentials with $n > 7$.

The increased stability of the bcc phase relative to the fcc phase as \tilde{T} increases implies that the entropy of the bcc phase is higher. Zener¹⁴ suggested that this was a consequence of lower-frequency shear modes in the open bcc structure. Friedel¹⁵ noted that shear constants of bcc crystals are not anomalously low. He suggested that since there are fewer nearest neighbors in the bcc structure the phonon energies are lower. However, at constant density the nearest-neighbor distance is shorter in the bcc structure, and the six next-nearest neighbors are only 17% farther away. Indeed, Eq. (3) implies that $\langle \omega_{\text{bcc}}^2 \rangle > \langle \omega_{\text{fcc}}^2 \rangle$ for $\lambda > 1.72$ where the fcc phase has the lower energy. For the Yukawa potential the lowest energy phase always has a higher entropy in the Einstein approximation, suggesting that it should remain stable as T increases.

To examine the source of the entropy difference which drives the fcc to bcc transition, the phonon spectrum was calculated as a function of λ for both structures. In the quasiharmonic approximation the entropy difference is given by

$$\Delta S = S_{\text{bcc}} - S_{\text{fcc}} = N^{-1} \sum_j \ln(\omega_{\text{fcc}}^j / \omega_{\text{bcc}}^j), \quad (4)$$

where the sum is over all normal modes. Trends in ΔS and $\langle \omega_{\text{fcc}}^2 \rangle / \langle \omega_{\text{bcc}}^2 \rangle$ may be different because they represent different averages over normal modes. We find, as suggested by Zener,¹⁴ that $\Delta S > 0$ because the shear modes in the bcc structure are softer. For λ between 2 and 5 the sound velocities of shear modes are about 50% smaller in the bcc structure. As $\lambda \rightarrow 7.67$ the shear velocity in

the bcc phase goes to zero and the structure becomes unstable.

The fcc-bcc phase boundary calculated in the quasiharmonic approximation is indicated by the dotted line in Fig. 1. The solid line is a guide to the eye interpolating between our MD results. In the low-temperature limit the quasiharmonic approximation becomes exact and the two lines converge. Anharmonic terms become important at higher \tilde{T} , and the range of stability of the bcc phase is sharply decreased from the quasiharmonic result.¹⁶ No evidence for the effect suggested by Alexander and McTague is seen.

Our results for the melting transition provide a test of phenomenological rules such as those of Hansen and Verlet³ and Lindemann.⁴ Since the potential shape varies continuously with λ , any deviations from these rules can be studied closely. We have determined the value of $\langle \delta u^2 \rangle \equiv \langle |r_i(t) - \langle r_i(t) \rangle|^2 \rangle$ (Lindemann) and the peak heights of $S(k)$ (Hansen-Verlet) and $g(r)$ in a range of temperatures around the lowest temperature where a solid starting state melted.¹⁷ We assume that the true melting temperature is about 15% below these points as found by Pollock and Hansen⁸ for $\lambda=0$. (The trends described below are seen for any uniform assumption about the difference between T_c and the temperature where melting is observed.)

The peak value of $g(r)$ at melting varies substantially from about 2.3 for $\lambda=2$ to 2.7 for $\lambda=12$. This range corresponds to a change in \tilde{T} of about 50% of \tilde{T}_c at a given λ . The variation of the peak in $g(r)$ reflects the dramatic change in the shape of the potential. For larger λ , the anharmonic components of the potential limit the closest separation of two particles more than at smaller λ . This leads to a sharpening of the nearest-neighbor peak and a larger peak height at comparable values of \tilde{T}/\tilde{T}_c .

According to the Hansen-Verlet rule³ the height of the

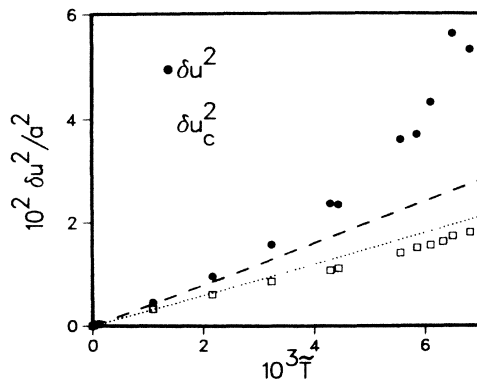


FIG. 2. The variation of $\langle \delta u^2/a^2 \rangle$ and the displacement relative to nearest neighbors δu_c^2 with \tilde{T} , for $\lambda=5$. The dashed and dotted lines show the respective quantities in the harmonic approximation.

first peak in $S(k)$ for a cooled liquid reaches 2.85 at the melting temperature. We find that the peak height is always near this value (± 0.2) at melting. However, there appears to be a systematic decrease in the peak height at melting as λ increases. More accurate simulations are underway to test this observation and to correlate it with the variation in the peak height in $g(r)$.

We found that the Lindemann criterion gave the closest correlation with the melting transition. The melting curve (dashed line) indicated in Fig. 1 gives the value of \tilde{T} where $(\delta u^2/a^2)^{1/2}$ was equal to 19%, for the relevant solid structure.¹⁸ Within our accuracy ($\sim 3\%$) the MD results fall on a straight line which lies about 15% below the upper bound for T_c set by the melted runs, and tracks these results over the entire range of λ . Pollock and Hansen⁸ found this value at the melting temperature for $\lambda=0$, and the value at melting for other potentials is very close.¹⁹

The melting curve in Fig. 1 is strongly affected by changes in the phonon spectrum and anharmonic terms as λ varies.⁹ If the phonon spectra and anharmonic terms simply scaled with ω_E the melting line would be horizontal.^{7,16} The melting line predicted by the low- T quasiharmonic theory increases monotonically by a factor of 2 over the range of λ shown. However, the rate of increase is not as fast as in the MD results. As λ increases, anharmonic effects become stronger and increase the value of \tilde{T} at melting.

The Lindemann criterion for normal metals is usually evaluated from a Debye-model fit to the low-temperature specific heat. Melting is found when the predicted value of $\langle \delta u^2/a^2 \rangle^{1/2}$ is between 0.07 and 0.10. It is not clear whether this range of values reflects a real varia-

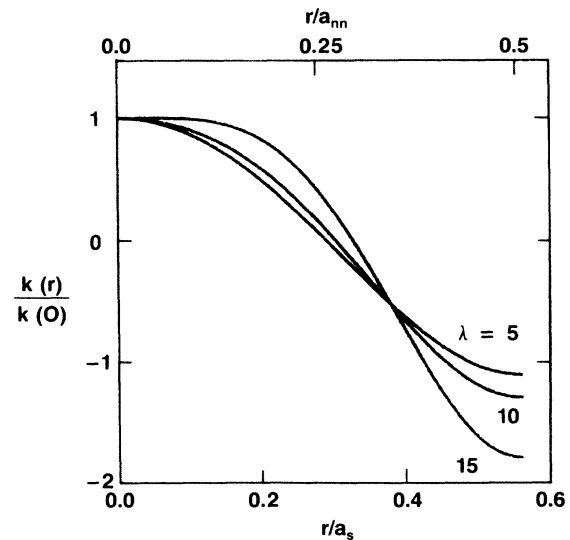


FIG. 3. The normalized force constant for lines of atoms displaced along the [110] direction as a function of their displacement relative to the lattice, for the indicated values of λ .

tion in $\langle \delta u^2/a^2 \rangle$ or the inadequacy of a harmonic Debye model. Our results are consistent with the latter conclusion. We find a constant value of $\langle \delta u^2/a^2 \rangle$ at melting, and that anharmonic terms and the shape of the phonon spectrum can vary $\langle \delta u^2/a^2 \rangle$ by more than a factor of 2.

Figure 2 shows the variation of $\langle \delta u^2/a^2 \rangle$ with temperature for $\lambda=5$. For low \tilde{T} , $\langle u^2/a^2 \rangle$ varies linearly with \tilde{T} as predicted by the quasiharmonic theory. As \tilde{T} approaches \tilde{T}_c the value of $\langle \delta u^2/a^2 \rangle$ rises more rapidly, making it easy to pinpoint \tilde{T}_c . It may seem surprising that $\langle \delta u^2/a^2 \rangle$ increases more rapidly than predicted by the harmonic theory. Since volume is held fixed and the interparticle potential is steeper as the particles move closer, one expects the anharmonic terms to limit $\langle \delta u^2/a^2 \rangle$. In fact, if one plots the mean displacement of a site relative to the center of mass of its nearest neighbors (Fig. 2), one finds this quantity does increase more slowly than \tilde{T} . The large values of $\langle \delta u^2/a^2 \rangle$ arise from correlated motion of many atoms.

To explore the nature of the anharmonic terms we calculated the energies of lines of atoms displaced along the line relative to the remainder of an fcc crystal. In Fig. 3 the effective force constant, normalized to the value at zero displacement, is plotted as a function of displacement for the [110] direction. The force constant decreases with displacement indicating that anharmonic terms actually soften the interaction. This explains the increase in $\langle \delta u^2/a^2 \rangle$ relative to the harmonic theory. When the atoms are displaced by the interparticle spacing along the line, the energy has returned to its original value. Thus for some range of displacements the second derivative must decrease. For the close-packed [110] direction this softening begins at zero displacement for $\lambda < 13$. The value of λ where the effect of anharmonic effects changes sign is smaller for less close-packed lines.⁹

In conclusion, we have determined the phase diagram for one of the classic interparticle potentials, the Yukawa potential. This phase diagram should prove useful for comparison with experiments as well as for provision of tests for analytical calculations of phase diagrams, such as those in the density-functional theories of freezing.

We thank S. Alexander, P. Chaikin, P. Pincus, and N. Clark for useful discussions. One of us (M.O.R.) acknowledges National Science Foundation support through Grant No. DMR-85-53271.

Mainz, D-6500 Mainz, West Germany.

^(b)Permanent address: Department of Physics and Astronomy, Johns Hopkins University, Baltimore, MD 21218.

¹P. Pieranski, *Contemp. Phys.* **24**, 25 (1983); W. van Meegen and I. Snook, *Adv. Colloid Interface Sci.* **21**, 119 (1984); P. M. Chaikin, J. M. diMeglio, W. D. Dozier, H. M. Lindsay, and D. A. Weitz (to be published).

²B. J. Ackerson and N. Clark, *Phys. Rev. Lett.* **46**, 123 (1981).

³L. Verlet, *Phys. Rev.* **165**, 201 (1968); J. P. Hansen and L. Verlet, *Phys. Rev.* **184**, 150 (1969).

⁴F. A. Lindemann, *Z. Phys.* **11**, 609 (1910).

⁵See, for example, R. Hultgren, R. L. Orr, P. D. Anderson, and K. K. Kelley, *Selected Values of Thermodynamic Properties of Metals and Alloys* (Wiley, New York, 1963).

⁶S. Alexander, P. M. Chaikin, P. Grant, G. J. Morales, P. Pincus, and D. Hone, *J. Chem. Phys.* **80**, 5776 (1984).

⁷D. Hone, S. Alexander, P. M. Chaikin, and P. Pincus, *J. Chem. Phys.* **79**, 1474 (1983).

⁸E. L. Pollock and J. P. Hansen, *Phys. Rev. A* **8**, 3110 (1973).

⁹M. O. Robbins, K. Kremer, and G. Grest, to be published. While the lattice sums which determine the stable phase at $\tilde{T}=0$ are affected by truncation of the potential, the free energy at finite \tilde{T} is less sensitive because $g(r)$ is smoothed out.

¹⁰M. Parrinello and A. Rahman, *Phys. Rev. Lett.* **45**, 1196 (1980).

¹¹A. Rahman and G. Jacucci, *Nuovo Cimento* **4D**, 357 (1984).

¹²S. Alexander and J. P. McTague, *Phys. Rev. Lett.* **41**, 702 (1978).

¹³W. G. Hoover, D. A. Young, and R. Grover, *J. Chem. Phys.* **56**, 2207 (1972).

¹⁴C. Zener, *Phys. Rev.* **71**, 846 (1947), and in *Phase Stability in Metals and Alloys*, edited by P. S. Rudman, J. Stringer, and R. I. Jaffee (McGraw-Hill, New York, 1967), p. 25.

¹⁵J. Friedel, *J. Phys. (Paris), Lett.* **35**, L59 (1974).

¹⁶Note that the self-consistent Einstein model used in Ref. 7 predicts that anharmonic terms increase bcc stability. This calculation produces several other qualitatively incorrect predictions and the calculated melting temperature was too high by a factor of about 8.

¹⁷Preliminary Monte Carlo studies of the temperature dependence of $g(r)$ for particles interacting with a Yukawa potential are described in W. Van Meegen and I. K. Snook, *J. Chem. Phys.* **66**, 813 (1977).

¹⁸Note that there will be coexistence regions separating the liquid and solid phases and the two solid phases. These regions are too small for us to detect with the MD techniques described here.

¹⁹J. P. Hansen and I. R. McDonald, *Theory of Simple Liquids* (Academic, New York, 1976). Note that the displacement δu is often referenced to the nearest-neighbor spacing rather than a .

^(a)Permanent address: Institut für Physik, Universität